Article

Side Reactions in Controlling the Quality, Yield, and Stability of High Quality Colloidal Nanocrystals

Yongfen Chen, Myeongseob Kim, Guoda Lian, Mathew B. Johnson, and Xiaogang Peng

J. Am. Chem. Soc., **2005**, 127 (38), 13331-13337• DOI: 10.1021/ja053151g • Publication Date (Web): 30 August 2005

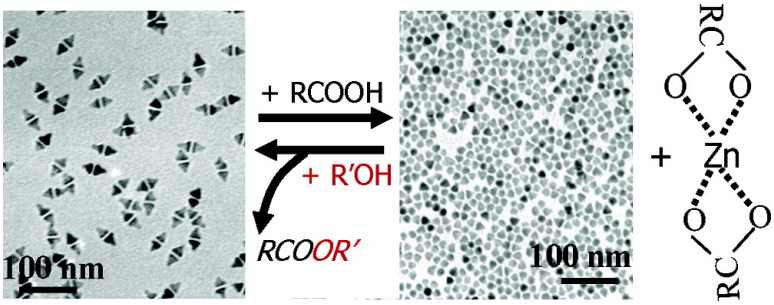

More About This Article

Additional resources and features associated with this article are available within the HTML version:

- Supporting Information
- Links to the 17 articles that cite this article, as of the time of this article download
- Access to high resolution figures
- Links to articles and content related to this article
- Copyright permission to reproduce figures and/or text from this article

View the Full Text HTML

J|A|C|S
ARTICLES
Published on Web 08/30/2005

Side Reactions in Controlling the Quality, Yield, and Stability of High Quality Colloidal Nanocrystals

Yongfen Chen,[†,‡] Myeongseob Kim,[†,‡] Guoda Lian,[‡,§] Mathew B. Johnson,[‡,§] and Xiaogang Peng*[,†,‡]

Contribution from the Department of Chemistry and Biochemistry, University of Arkansas, Fayetteville, Arkansas 72701, Joint MRSEC at the University of Oklahoma and the University of Arkansas, and Department of Physics and Astronomy, University of Oklahoma, Norman, Oklahoma 73019

Received May 13, 2005; E-mail: xpeng@uark.edu

Abstract: Effects of side reactions during the formation of high quality colloidal nanocrystals were studied using ZnO as a model system. In this case, an irreversible side reaction, formation of esters, was identified to accompany formation of ZnO nanocrystals through the chemical reaction between zinc stearate and an excess amount of alcohols in hydrocarbon solvents at elevated temperatures. This irreversible side reaction made the resulting nanocrystals stable and with nearly unity yield regardless of their size, shape, and size/shape distribution. Ostwald ripening and intraparticle ripening were stopped due to the extremely low solubility/stability of the possible monomers because all free ligands in the solution were consumed by the side reaction. However, focusing on size distribution and 1D growth that are needed for the growth of high quality nanocrystals could still occur for high yield reactions. Upon the addition of a small amount of stearic acid or phosphonic acid, immediate partial dissolution of ZnO nanocrystals took place. Although the excess alcohol could not react with the resulting zinc phosphonic acid salt, it could force the newly formed zinc stearate gradually but completely back onto the existing nanocrystals. The results in this report indicate that side reactions are extremely important for the formation of high quality nanocrystals by affecting their quality, yield, and stability under growth conditions. Due to their lack of information in the literature and obvious practical advantages, studies of side reactions accompanying formation of nanocrystals are important for both fundamental science related to crystallization and industrial production of high quality nanocrystals.

Introduction

Synthesis of high quality colloidal nanocrystals has advanced dramatically in the past few years. For this substantial change, the broad interest on colloidal nanocrystals has created necessary momentum, and significant knowledge accumulated through systematic chemical kinetic and structural studies has provided a needed foundation. Synthesis of high quality nanocrystals often occurs in a complex solution system, and many side reactions may thus accompany the formation of nanocrystals, which is likely one of the reasons many existing synthetic schemes are difficult to reproduce. To our knowledge, the effects of side reactions are poorly addressed. In most cases, including classic studies of growth mechanisms of colloidal nanocrystals,[1−3] side reactions are often not considered, although significant attention has been paid to the effects of ligands,[1−3] surface moieties,[4,5] and recently also to the activation reagents.[6,7] In classic crystallization, side reactions have hardly been mentioned, either.[8]

This work will report some interesting and dramatic effects of side reactions, especially irreversible ones, on the formation of high quality nanocrystals using shape-controlled ZnO nanocrystals as the model system. The results indicate that nearly all processes in crystallization, including nucleation, growth, dissolution, and Ostwald as well as other ripening processes, can be closely coupled with side reactions. To an extreme, any of these processes can be completely turned on or off upon manipulating side reactions under given growth conditions.

Shape-controlled growth of crystals in solution has traditionally been called crystal habits and has been explained by two models, Wuff facet theory and surface additive mediated growth,[8] which are also applied for explaining the growth of colloidal nanocrystals and nanostructures.[4,5,9−12] Growth of high

† University of Arkansas.
‡ Joint MRSEC.
§ University of Oklahoma.

(1) Murray, C. B.; Norris, D. J.; Bawendi, M. G. *J. Am. Chem. Soc.* **1993**, *115*, 8706−8715.
(2) Peng, X.; Wickham, J.; Alivisatos, A. P. *J. Am. Chem. Soc.* **1998**, *120*, 5343−5344.
(3) Peng, Z. A.; Peng, X. *J. Am. Chem. Soc.* **2001**, *123*, 1389−1395.
(4) Herricks, T.; Chen, J.; Xia, Y. *Nano Lett.* **2004**, *4*, 2367−2371.
(5) Im, S. H.; Lee, Y. T.; Wiley, B.; Xia, Y. *Angew. Chem., Int. Ed.* **2005**, *44*, 2154−2157.
(6) Jana, N. R.; Chen, Y.; Peng, X. *Chem. Mater.* **2004**, *16*, 3931−3935.
(7) Li, L. P., N.; Wang, Y.; Peng, X. *Nano Lett.* **2004**, *4*, 2261−2264.
(8) Mullin, J. W. *Crystallization*, 3rd ed.; Butterworth-Heinemann: Oxford, 1997.
(9) Murphy, C. J.; Jana, N. R. *Adv. Mater.* **2002**, *14*, 80−82.
(10) Pileni, M.-P. *Nat. Mater.* **2003**, *2*, 145−150.
(11) Li, F.; Ding, Y.; Gao, P.; Xin, X.; Wang, Z. L. *Angew. Chem., Int. Ed.* **2004**, *43*, 5238−5242.

quality nanocrystals needs a substantially more amount of knowledge on crystallization. This is so because colloidal nanocrystals must be controlled by not only their size and shape but also size and shape distribution in order to exploit their size-dependent properties. Studies of nanocrystal growth have revealed several new routes, such as template directed,[13−16] oriented attachment,[17,18] photoradiation induced growth,[19] and monomer activity mediated growth for shape-controlled growth.[20] Monomer activity mediated growth of high quality II−VI semiconductor nanocrystals has been well documented, and the related mechanisms have become more and more clear[3,20−24] since the first few reports on the control of their size/size distribution and later shape/shape distribution of the nearly monodisperse CdSe nanocrystals in quantum confinement size regime were reported. This mechanism has been regarded as the most valuable model system in the field of colloidal nanocrystals. For this reason, a brief discussion about this model system is given as follows.

The synthesis is typically performed in nonaqueous solutions under elevated temperatures. Overall, ligands in these reaction systems assist the symmetry broken of a given crystal structure, which provides the intrinsic requirement for the growth of nonequilibrium shapes. Ligands further play a key role in manipulating the activity coefficient of the monomers in solution, which in turn controls the relative nucleus concentration in the solution. If a relatively high remaining monomer concentration and a low nucleus concentration can be managed in the growth phase, thermodynamic unfavorable shapes, such as rods, rices, branched ones, etc., will become accessible to the system and nonequilibrium shaped nanocrystals can thus be formed with the strong thermodynamic overdriving provided by the high remaining monomer concentration. However, when the monomer concentrations are gradually depleted to a certain level due to the growth of the nanocrystals, the thermodynamic unfavorable shapes become not stable and have been observed to evolve into the equilibrium shape, dots, through intraparticle ripening.[3] Experimental data imply that a low monomer concentration not only destabilizes the nonequilibrium shapes but also induces Ostwald ripening among dot-shaped nanocrystals or defocusing of size distribution.[2]

The above discussions imply that, fundamentally, reasonably high remaining monomer concentrations are needed for the growth of monodisperse nanocrystals, especially for nonequilibrium shaped ones. However, a high monomer concentration in solution means that the conversion ratio of monomers, or yield, is low (less than 50% for known II−VI semiconductor nanocrystals with elongated shapes).[3,21,24] Practically, such reactions must be stopped within a very small time window. An early stop would end up with a differently sized and/or shaped nanocrystal sample, and an elongated reaction would yield nanocrystals with a broad size distribution because of Ostwald ripening (or defocusing of size distribution) and intraparticle ripening as discussed above.

Growth of high quality ZnO nanocrystals is chosen as the model system for studying side reaction effects. Synthesis of ZnO nanocrystals/nanostructures has attracted significant attention in the recent years because of its potential as UV emitting materials, catalysts, host materials for doped nanocrystals, etc.[11,12,18,25−32] Despite all of the progress, nearly monodisperse and shape-controlled ZnO nanocrystals with pure band gap emission are still hard to obtain. In addition, formation of ZnO nanocrystals can be carried out in a very simple system, as described below, which makes it ideal for studying the effects of side reactions.

Results and Discussion

Growth of ZnO nanocrystals through the reaction of zinc stearate with alcohol in hydrocarbon solvents (noncoordinating solvents) under elevated temperatures is chosen as our model system. This system is developed on the basis of the synthetic scheme designed for magnetic oxide nanocrystals reported recently.[6] The resulting nanocrystals in this system were stable at room temperature, and no aggregation or oriented attachment[17,18] was observed. The reaction scheme and the resulting nanocrystals at different stages are illustrated in Figure 1.

Zinc stearate was found to be stable in hydrocarbon solvents with the reaction temperature up to 320 °C. The FTIR spectrum (Figure 1, right panel) before the addition of the alcohol was dominated by the $-CH_2-$ vibration (the strongest band at 1466 cm^{-1} in all FTIR spectra) and $-COO^-$ asymmetric vibration (the second strongest one, 1536 cm^{-1}) in the 1000−2000 cm^{-1} spectrum window. However, with alcohol added in, zinc stearate immediately became unstable and it decomposed quite rapidly. The completion of the reaction is evidenced by the FTIR spectra (the second and fourth spectra from the top in Figure 1). For instance, a few minutes after the addition of the alcohol, the $-COO^-$ asymmetric vibration peak decreased by about 95% (relative to the $-CH_2-$ vibration band), and an ester $-C{=}O$ vibration band (1730 cm^{-1}) appeared (the second spectrum from the top in Figure 1). After careful purification, we verified that stearate is the surface ligand for the resulting ZnO nanocrystals (see Supporting Information), which means that a small portion of the remaining 5% of the $-COO^-$ asymmetric vibration peak in the second spectrum from the top in Figure 1 (right panel)

(12) Tian, Z. R.; Voigt, J. A.; Liu, J.; McKenzie, B.; McDermott, M. J.; Rodriguez, M. A.; Konishi, H.; Xu, H. *Nat. Mater.* **2003**, *2*, 821−826.
(13) Nishizawa, M.; Menon, V. P.; Martin, C. R. *Science* **1995**, *268*, 700−702.
(14) Trentler, T. J.; Hickman, K. M.; Goel, S. C.; Viano, A. M.; Gibbons, P. C.; Buhro, W. E. *Science* **1995**, *270*, 1791−1794.
(15) Han, W.; Fan, S.; Li, Q.; Hu, Y. *Science* **1997**, *277*, 1287−1289.
(16) Gates, B.; Wu, Y.; Yin, Y.; Yang, P.; Xia, Y. *J. Am. Chem. Soc.* **2001**, *123*, 11500−11501.
(17) Penn, R. L.; Banfield, J. F. *Science* **1998**, *281*, 969−971.
(18) Pacholski, C.; Kornowski, A.; Weller, H. *Angew. Chem., Int. Ed.* **2002**, *41*, 1188−1191.
(19) Jin, R.; Cao, Y. C.; Hao, E.; Metraux, G. S.; Schatz, G. C.; Mirkin, C. A. *Nature* **2003**, *425*, 487−490.
(20) Peng, X.; Manna, U.; Yang, W.; Wickham, J.; Scher, E.; Kadavanich, A.; Allvisatos, A. P. *Nature* **2000**, *404*, 59−61.
(21) Peng, Z. A.; Peng, X. *J. Am. Chem. Soc.* **2002**, *124*, 3343−3353.
(22) Lee, S.-M.; Cho, S.-N.; Cheon, J. *Adv. Mater.* **2003**, *15*, 441−444.
(23) Manna, L.; Milliron, D. J.; Meisel, A.; Scher, E. C.; Alivisatos, A. P. *Nat. Mater.* **2003**, *2*, 382−385.
(24) Yu, W. W.; Wang, Y. A.; Peng, X. *Chem. Mater.* **2003**, *15*, 4300−4308.
(25) Huang, M. H.; Mao, S.; Feick, H.; Yan, H.; Wu, Y.; Kind, H.; Weber, E.; Russo, R.; Yang, P. *Science* **2001**, *292*, 1897−1899.
(26) Shim, M.; Guyot-Sionnest, P. *J. Am. Chem. Soc.* **2001**, *123*, 11651−11654.
(27) Radovanovic, P. V.; Norberg, N. S.; McNally, K. E.; Gamelin, D. R. *J. Am. Chem. Soc.* **2002**, *124*, 15192−15193.
(28) Greene, L. E.; Law, M.; Goldberger, J.; Kim, F.; Johnson, J. C.; Zhang, Y.; Saykally, R. J.; Yang, P. *Angew. Chem., Int. Ed.* **2003**, *42*, 3031−3034.
(29) Radovanovic, P. V.; Gamelin, D. R. *Phys. Rev. Lett.* **2003**, *91*, 157202/1−157202/4.
(30) Schwartz, D. A.; Norberg, N. S.; Nguyen, Q. P.; Parker, J. M.; Gamelin, D. R. *J. Am. Chem. Soc.* **2003**, *125*, 13205−13218.
(31) Yin, M.; Gu, Y.; Kuskovsky, I. L.; Andelman, T.; Zhu, Y.; Neumark, G. F.; O'Brien, S. *J. Am. Chem. Soc.* **2004**, *126*, 6206−6207.
(32) Norberg, N. S.; Kittilstved, K. R.; Amonette, J. E.; Kukkadapu, R. K.; Schwartz, D. A.; Gamelin, D. R. *J. Am. Chem. Soc.* **2004**, *126*, 9387−9398.

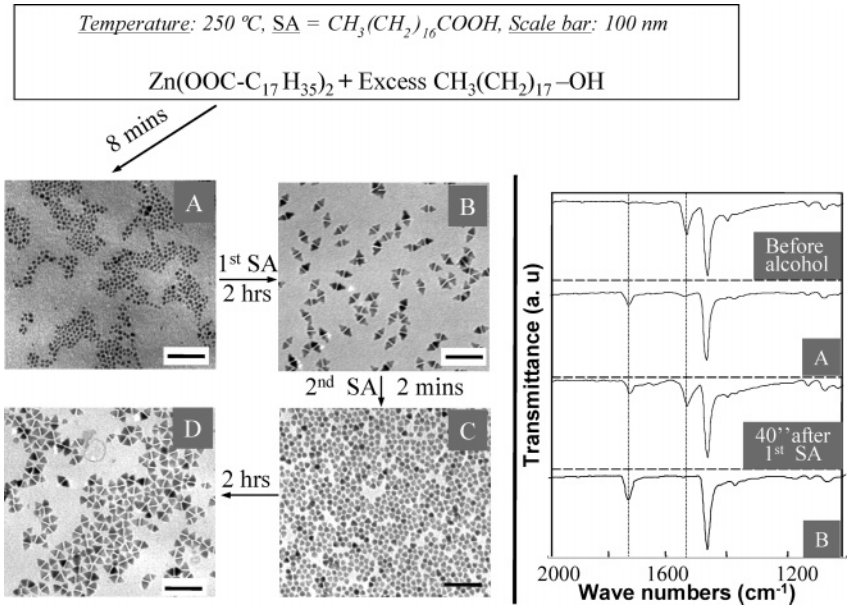

Figure 1. Left: Size and shape evolution of ZnO nanocrystals demonstrated by TEM images (see text for reaction conditions). Right: FTIR spectra of the reaction mixture taken at different stages.

should come from the surface ligands. The ^1H NMR spectra of the ester and the surface ligands are provided in Supporting Information.

The initial nanocrystals formed by this reaction were faceted wurtzite nanocrystals with a relatively broad size and shape distribution (Figure 1, image A). However, the size, shape, and size/shape distribution of the nanocrystals revealed by TEM measurements, the UV−vis absorption spectrum, and the FTIR spectrum did not change upon further heating for as long as 7 h. The mass yield counted by zinc atoms was determined to be approximately 100%. This was consistent with the results obtained using the standard methods for determining metal ion (Zn^{2+}) concentration by atomic absorption (see Experimental Section). The average conversion ratio for zinc stearate to zinc oxide nanocrystals was determined to be 96% (see details in the Supporting Information). This indicates that, after the precursors were consumed completely, nanocrystals, despite their different size and shape in this specific system, are stable for a high yield reaction.

A reasonable hypothesis for the unusual stability of the resulting nanocrystals discussed in the above paragraph is as follows. After all precursors were consumed, growth of the nanocrystals could only occur through Ostwald ripening. Ostwald ripening basically occurs by dissolving the monomers from relatively small nanocrystals into solution and growing them back onto relatively large ones among the distribution. However, there were no free ligands in the solution for stabilizing the monomers in this case, indicated by the FTIR spectrum. The ultimate instability of the monomers, because of a lack of ligands, should thus make Ostwald ripening impossible. This hypothesis was tested by introducing some free ligands, fatty acids, into the reaction system.

Although the nanocrystals as well as the entire reaction system were stable for hours under the above conditions, some dramatic changes were observed when stearic acid was introduced into the reaction system. The nanocrystals were eventually converted to stable pyramid-shaped ones, nanopyramids, which appeared triangular in TEM images (images B and D in Figure 1, and

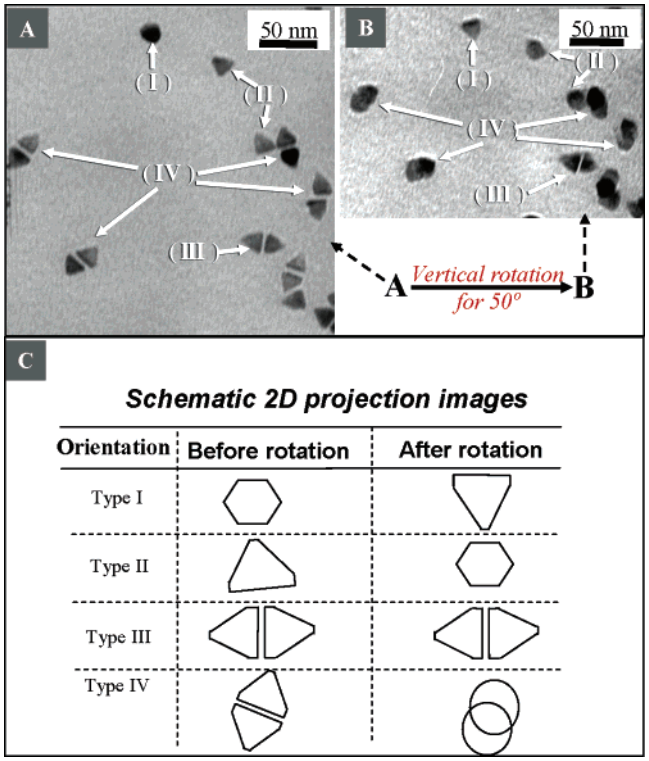

Figure 2. TEM images of nanocrystals before (A) and after (B) the rotation; (C) summaries of the morphology evolution of differently oriented nanocrystals.

Figure 2). The stable nanopyramids became unstable again if additional fatty acids were added into the reaction solution.

Careful examination of the temporal evolution of the particle morphology revealed that the addition of fatty acids into the reaction solution of the nanopyramids converted the nanopyramids (image B, Figure 1) into relatively small dot-shaped ones (image C, Figure 1), and then, these dot-shaped nanocrystals grew back to stable nanopyramids (image D, Figure 1). This nanopyramid−nanodot−nanopyramid transition could be repeated for several cycles if the total number of moles of stearate

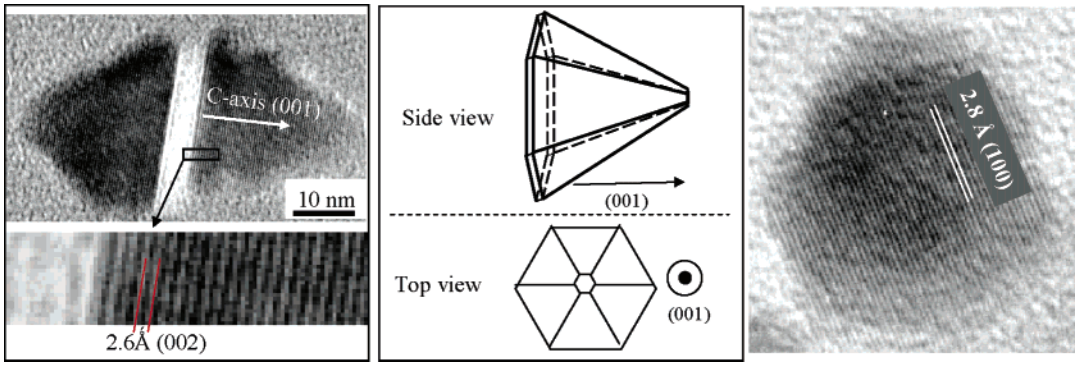

Figure 3. High-resolution TEM images and schematic illustration of the three-dimensional structure of the nanopyramids.

from the initial zinc stearate and the stearic acid added afterward was not more than the alcohol originally injected in.

The size of the pyramids after each dissolution−growth cycle could be varied by adding a different amount of stearic acid. The initial and final shape and average size of the nanopyramids remained approximately the same after the given cycle of shape evolution shown in Figure 1 (images B and D). To our knowledge, this is the first observation of reversible shape evolution without changing both the size and shape of nearly monodisperse nanocrystals. It should be pointed out that this shape evolution could not be considered to be reversible if the side reactions were taken into account (see more discussion below).

If significantly more stearic acid was added into the system with a sufficient amount of alcohol in the solution, the average size of the pyramids could also be bigger than the initial ones. This was similar to the initial etching−regrowth cycle shown in Figure 1 (from image A to image B). When stearic acid was added into the solution, monomer concentration was suddenly increased by dissolution of ZnO nanocrystals, with some of them partially dissolved and some—presumably small ones—completely dissolved. This replenishment of monomers brought the reaction system to "refocusing of size distribution", which is similar to secondary injections performed for regular high temperature synthesis. As a result, the pyramids were re-formed gradually by the reaction of alcohol and newly formed zinc stearate with a nearly monodisperse size distribution (image B), although the initial irregular nanocrystals (image A) were small and had a broad size distribution.

If the amount of stearic acids was in large excess and there was not enough alcohol in the solution, the nanocrystals would be smaller. Further increasing the amount of stearic acid would dissolve all nanocrystals permanently.

FTIR spectra revealed that the shape evolution illustrated in Figure 1 was accompanied by the relative intensity change of the carboxylate and the ester vibration bands. All stearic acid added into the system was converted to zinc stearate almost instantaneously (the third FTIR spectrum from the top, Figure 1). This indicates that stearic acid dissolved ZnO nanocrystals rapidly, which is consistent with the size decrease of the transition-state (dot-shaped) nanocrystals (comparing image C with images B and D, Figure 1). When the nanocrystals grew back to pyramids (image D, Figure 1), the vibration band of the carboxylate group disappeared and the intensity of the ester vibration band increased in comparison to the $-CH_2-$ reference band at 1466 cm^{-1} (spectrum B, Figure 1). This implies that the shape evolution cycle was accompanied by the formation of esters by the fatty acids added in and the existing excess alcohol in the reaction solution. As pointed out above, the ^1H NMR spectrum of the resulting ester is provided in the Supporting Information. In a sense, ZnO nanocrystals acted as "catalysts" or "templates" for the irreversible formation of the esters.

The shape of the nanocrystals in images B and D in Figure 1 is confirmed to be pyramid-shaped, although their two-dimensional (2D) projection in TEM images looks triangular. This is determined by rotating the TEM grid along a fixed axis (Figure 2).

High-resolution TEM images (Figure 3) revealed that the *c*-axis of the wurtzite structure is perpendicular to the basal plane of the pyramids (indices of the facets are available in the Supporting Information). Nanopyramids intended to pack in pairs, which is better evident in image B in Figure 1 and also in Figure 2. This tendency seems to be caused by the well-developed facet of the basal plane (Figure 3, right), which is also the slow growth facet (see more discussion later). In comparison, the lateral facets of the nanopyramids are not perfectly developed, although each nanopyramid is a single crystal (Figure 3). As pointed out by one of the reviewers, the pyramids should be polarized, with the dipole moment perpendicular to the basal plane. If the basal plane could be terminated by either zinc or oxygen ions, two differently charged pyramids could attract each other through the opposite charges at their basal plane and form pairs. Further evidences are needed to decisively interpret the pair formation.

The transition dot-shaped nanocrystals from the initial pyramids to the next one were typically not very spherical, often mixed with some small pyramids (Figure 1, image C). This is likely because there was an excess amount of alcohol in the solution and some growth always accompanied the dissolution process although the growth reaction was substantially slower, as revealed by TEM and FTIR measurements (Figure 1). To confirm this, octadecylphosphonic acid (ODPA) was used in place of stearic acid. As a result, almost perfectly dot-shaped nanocrystals with good size distribution could be obtained as stable products (Figure 4, top). This is so because Zn phosphonic salts are stable under the reaction conditions, even with a large amount of alcohol in the solution. It should be pointed out that, although these dot-shaped nanocrystals were stable under the growth conditions, the yield of these nearly monodisperse dot-shaped nanocrystals was below unity because of the stability of zinc phosphonic salts.

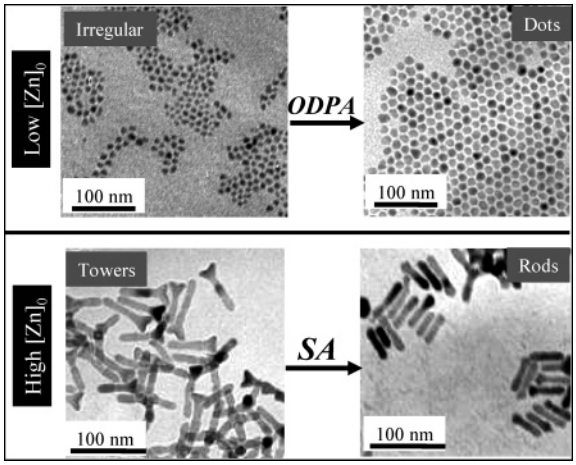

Figure 4. Top: Formation of stable dot-shaped nanocrystals. Only initial nanocrystals (left) and the final products (right) are shown, and the nearly monodisperse pyramid nanocrystals before addition of ODPA are similar to the ones shown in Figure 1. Bottom: Transition of tower-shaped nanocrystals to rod-shaped ones. $[Zn]_0$ refers to the initial zinc stearate concentration.

If a very high initial concentration of zinc stearate ($[Zn]_0$)—10 times higher than that of the typical reaction—was used, stable tower-shaped nanocrystals were formed (Figure 4, bottom left). This concentration-dependent shape is similar to that observed for CdSe and other II−VI semiconductor nanocrystals through low yield reactions that high monomer concentrations yield elongated nanocrystals.[3,20,21,23,24] Similar to the results discussed above, these tower-shaped nanocrystals were found to be stable under the reaction conditions after the consumption of all monomers. This result means that reversible side reactions can also stabilize elongated nanocrystals.

If a small amount of stearic acid was added into the tower-shaped nanocrystal solution, the nanocrystals became rods by shortening the length and removing the small fin-ring around the basal plane of the nanotowers (Figure 4, bottom right). Further heating of these rods with the presence of an excess amount of alcohol would form a mixture of towers, rods, and some pyramids. The appearance of the new shape, pyramids, is likely a result of the secondary nucleation and growth caused by the regenerated zinc stearate.

The shape evolution and shape-controlled growth of ZnO nanocrystals discussed above are summarized in Figure 5 (top panel). Although the thermodynamically stable shape for wurtzite crystals should be a slightly elongated dot-shape,[1] the above results demonstrate that many different shapes, including the elongated ones, were extremely stable if no acids were added into the system. This confirms the hypothesis that, after precursors are consumed, a nanocrystal dispersion with any size and shape in a unity yield reaction shall remain as it is.

Because nanocrystals are thermodynamic metastable species, their exceptional stability observed in this system should be a kinetic phenomenon. This means that there is a kinetically prohibitive free energy barrier—a high activation energy—between two sets of size/shape distributions. For the shape transition between dots and pyramids, a simplified illustration of the reaction free energy curve is illustrated in Figure 5 (bottom).

From left to right, fatty acid is needed for the system to go through the dashed green line, a low activation energy path,

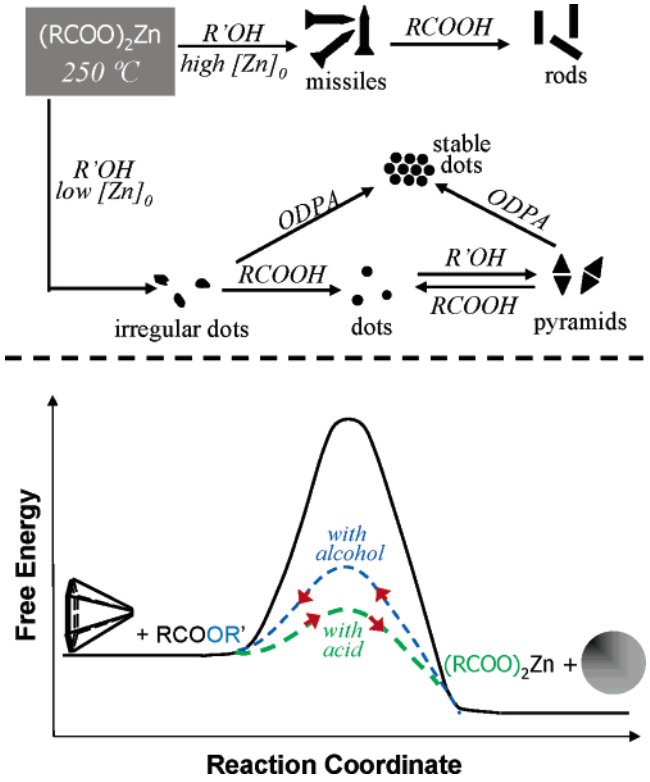

Figure 5. Top: Summary of shape evolution of ZnO nanocrystals. Bottom: Schematic illustration of the free energy diagram for the reversible shape transition without considering the free energy of organic species. The black solid line refers to the path going from left to right without acid and going from right to left without alcohol.

and reach spherical particles. Without acids, the kinetic barrier (black line, Figure 5 (bottom)) is simply too high to be overcome. Similarly, alcohol is needed to convert dot-shaped nanocrystals back to pyramids by going through the low activation path (dashed blue line). If no activation reagents, alcohol for this system going from right to left in the case of fatty acids used, the very high barrier (black solid line) will again make this conversion kinetically prohibitive under the given conditions. Because alcohols do not react with zinc phosphonic acid salts, existence of alcohol in the reaction system could not offer a lower activation energy as it did for the zinc fatty acid salts.

The formation of ester is a completely irreversible side reaction under the given conditions. This provides needed thermodynamic overdriving and warrants the unity yield for the decomposition of zinc stearate (from right to left, Figure 4 (bottom)). The formation of zinc stearate by the addition of the fatty acid (from left to right, Figure 4 (bottom)) is irreversible only if no alcohol exists in the system. ODPA makes the reaction from left to right—dissolution of ZnO nanocrystals—irreversible under the reaction conditions even with the existence of alcohol, and thus the reaction is not really a high yield reaction, with some zinc trapped as phosphonic salts, although the resulting nanocrystals were stable under the reaction conditions.

The above results and analysis indicate that Ostwald ripening (defocusing of size distribution)[2] and intraparticle ripening[3] could not occur in the current system if no free acids were added in. This is not surprising since these two phenomena need the growth reaction to be reversible with reasonably stable monomers as the intermediates. As discussed above, Ostwald ripening

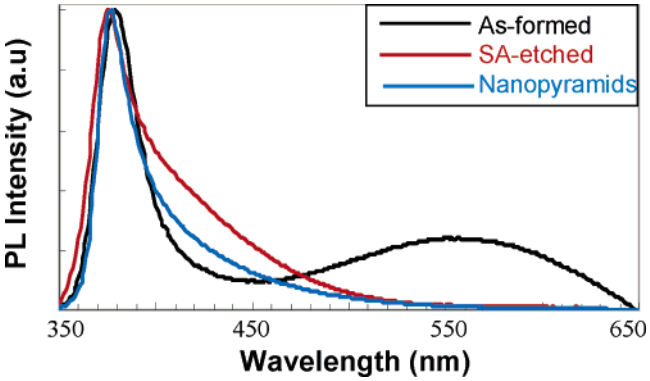

Figure 6. Photoluminescence (PL) spectra of ZnO nanocrystals at different stages.

basically occurs by dissolving monomers from the small nanocrystals in the solution and growing them back onto the relatively big nanocrystals in the same solution. This phenomenon can also be understood from another perspective. On the basis of the Gibbs−Thompson equation and its variation,[8,21] the solubilities of differently sized/shaped crystals will be the same if the bulk solubility is practically zero. This implies that all crystals, no matter what size/shape, are equally stable if the monomers cannot practically exist due to their extremely low stability. In a certain sense, a unity yield reaction should warrant a high stability of the resulting nanocrystals through simple reaction schemes, such as the model system studied here.

Growth of nonequilibrium shapes under high monomer concentrations[3,20] and focusing on size distribution[2] observed for II−VI semiconductor systems both seem to be applicable for this high yield system. This is reasonable because recent results indicate that these two processes only require high monomer concentration under diffusion-controlled conditions.[3]

The discussions offered here also provide an explanation why Ostwald ripening for the Au nanocrystals obtained through a synthetic scheme reported recently[33] could only occur with the addition of strong ligands, thiols. Similar to the system discussed here, the yield of Au nanocrystals in the specific scheme was observed to be nearly unity.[33]

Wuff facets theory suggests that crystal growth should occur rapidly on high free energy facets.[8] Experimental results in the nanometer regime further extended this thermodynamic argument to a kinetic version that dominating growth would be possible on high free energy facets under highly kinetic controlled growth conditions.[3] If these theories are applicable in the current system, the corners and the tip of pyramids should be high energy surfaces since the pyramids were reproducibly grown from more or less spherical nanocrystals (Figure 1). Interestingly, when acids were added in, these corners and the tip were "smoothed", which converted pyramids back to dots. This implies that dissolution of crystals may also occur preferably at high energy facets. This hypothesis is actually consistent with the photoluminescence (PL) results (Figure 6).

As shown in Figure 6, trap emission states that caused the low energy tail were largely removed by the acid etching and further reduced by the following growth process. The broad green emission band observed in the spectrum for the as-formed ZnO nanocrystals (black line) has been reported as the result of singly ionized oxygen traps.[28] This and other trap states of ZnO have been frequently observed for nanocrystals/nanostructures formed under various conditions,[26,28,31] which required harsh treatments to remove.[28] ZnO nanocrystals with nearly pure band gap emission should be of importance for their applications as UV emitters and as a host for doped nanocrystals. The results shown here further imply that photoluminescence properties of ZnO nanocrystals and other types of nanocrystals could be controlled by optimizing side reactions.

Conclusion

In summary, an irreversible side reaction, formation of ester, provides the needed thermodynamic driving force for the growth of ZnO nanocrystals with a high yield when fatty acids were used as the ligands for the nanocrystals and the monomers. The reversible dissolution and irreversible growth also made it possible for the nanocrystals to be reversibly converted from one shape to another and back to the original shape and size in a unity yield. The results confirmed that the two key concepts developed in studying II−VI semiconductor nanocrystals via low yield reactions, focusing of size distribution[2] and shape-selected growth under high monomer concentrations (such as 1D growth),[3] could still be exploited in high yield reactions. Irreversible side reactions make it possible to completely stop Ostwald ripening (defocusing of size distribution)[2] and intraparticle ripening[3] because of the extremely low stability/solubility of the monomers without proper free ligands in the solution. This makes the shape-controlled nanocrystals, both equilibrium shaped and nonequilibrium shaped ones, stable and with nearly unity yield in the reaction mixture. Therefore, it is not necessary to stop the growth reactions at a critical time window, as was usually needed for the existing schemes based on low yield reactions. The above features reveal that synthetic schemes of colloidal nanocrystals based on high yield reactions using generic chemicals are not only economically and environmentally attractive but also practical. Due to their lack of information in the literature of crystallization, side reactions deserve more systematic and quantitative studies. Such studies may provide some new clues for understanding crystallization in general.

Experimental Section

Materials. Zinc stearate and 1-octadecanol (97%) were purchased from Alfa Aesar; 1-octadecene (ODE, tech 90%), *n*-eicosane, and stearic acid (95%) were purchased from Aldrich, and octadecyl phosphoric acid (ODPA) was from Polycarbon Industries Inc. All chemicals were used without further purification.

If not specified, the reactions were all with free excess alcohol in the solution, and the reaction temperature was held as 250 °C for all processes, including etching by free fatty acids.

Synthesis of Nanopyramids and Shape Transition. Zinc stearate (0.2 mmol) and 4 g of 1-octadecene (ODE) were loaded in a 25 mL three-necked flask. The mixture was heated to 280 °C under Ar atmosphere. 1-Octadecanol (1 mmol) dissolved in 1 g of ODE at 200 °C was quickly injected into the zinc stearate solution, and the reaction temperature was then set at 250 °C throughout the entire synthesis. To synthesize ZnO nanopyramids, after the injection of 1-octadecanol for 8 min, stearic acid (0.2 mmol) dissolved in 0.5 g of ODE at 120 °C was injected into ZnO nanocrystals solution and incubated for 2 h. To convert the ZnO nanopyramids back to spherical particles, stearic acid (0.2 mmol) dissolved in 0.5 g of ODE at 120 °C was injected into the ZnO nanopyramids solution, and during the first few minutes after acid

(33) Jana, N. R.; Peng, X. *J. Am. Chem. Soc.* **2003**, *125*, 14280−14281.

injection, the shape of ZnO nanocrystals was spherical. The ZnO spherical shape eventually came back to nanopyramids after prolonged heating.

If 10 times more zinc stearate (2 mmol) was used, the reaction yielded nanotowers within a few minutes after the injection of 1-octadecanol. The tower-shaped nanocrystals were converted to nanorods by the addition of either stearic acids or ODPA following the same procedure described above.

Synthesis of Stable Dot-Shaped ZnO Nanocrystals. Stable dot-shaped ZnO nanocrystals were formed by the addition of 0.1 mmol 1-octadecanal phosphoric acid (ODPA) dissolved in 0.5 g of ODE into the ZnO nanopyramids solution at 250 °C and incubated for a few minutes.

Optical Measurements. Aliquots at different reaction stages were taken for TEM, UV, and FTIR measurements. UV−vis spectra were taken on a HP 8453 UV−visible spectrophotometer. Photoluminescence spectra were recorded on a Fluorolog-3 spectrofluorometer. Infrared spectra were obtained on a Nicolet Impact 410 spectrophotometer, and the specimens were prepared by dropping a hexane solution of ZnO nanocrystals on a NaCl crystal and dried in air. For FTIR measurements, *n*-eicosane was used as the solvent, instead of ODE, because of its simple FTIR spectrum in the 1000−2000 cm^{-1} window.

Transmission Electron Microscopy (TEM). TEM and high-resolution TEM images were taken on a JEOL X-100 at 100 kV and a JEOL 2010 at 300 kV, respectively. Specimens for JEOL X-100 were prepared by dipping a Formvar-coated copper grid into a toluene solution of the nanocrystals, and the grid with the nanocrystals was dried in air. Selected area electron diffraction pattern (SAED) was taken with a camera length of 120 cm. Specimen for JEOL 2010 at 300 kV were prepared by dipping a carbon-film-coated copper grid into a toluene solution of ZnO nanocrystals and dried in air.

Zinc Oxide Yield Determination. A. Purification of Zinc Oxide Nanocrystals for Yield Determination: Zinc oxide nanocrystals (0.2 mmol of zinc element) were synthesized through the same procedure as described above with the reaction time of 2 h. The zinc oxide nanocrystal solution was cooled to 50 °C; 20 mL of ethyl acetate was used to precipitate zinc oxide nanocrystals, and the nanocrystals were collected by centrifugation. Then the nanocrystals were dispersed in toluene, and any insoluble residue was removed by centrifugation. Zinc oxide nanocrystals were precipitated by methanol and collected by centrifugation. The zinc oxide nanocrystals were washed twice with methanol. The purified zinc oxide nanocrystals were dried in a vacuum oven at room temperature overnight. The weight of dried zinc oxide nanocrystals was 15.2 mg.

B. Zinc Oxide Nanocrystal Yield Determination by Atomic Absorption (AA): Zinc oxide nanocrystals were dispersed in 5 mL of toluene. To this solution, was added 1 mL of concentrated nitric acid, and the solution was sonicated for 1 min. Five milliliters of water was added into the digestion solution to extract zinc ions. The solution was centrifuged to separate water−toluene phases, and the toluene phase was discarded. Hexane (5 mL) was added to the aqueous solution containing zinc ion to further remove any organic residues. The hexane extraction process was repeated one more time. The resulting zinc ion solution was diluted with water to 8.1021 g.

Standard addition method was chosen to determine the zinc ion concentration, and 2.09 μg/mL (Cs = 2.09 μg/mL) zinc acetate solution was used as standard solution. Out of the zinc ion solution prepared above, 0.2224 g of solution was taken out and diluted with distilled water to 20.4073 g. Four aliquots of 0.5 mL of this diluted zinc ion solution were transferred into four vials, and to these solutions was added standard zinc ion solution, Vs = 0, 0.5, 1, and 1.5 mL, respectively. The solutions were further diluted to a total volume of 5 mL with distilled water. Atomic absorption was recorded on a GBC932 plus atomic absorption spectrometer.

Acknowledgment. Financial support from the National Science Foundation is acknowledged.

Note Added in Proof. After this work was accepted for publication, the authors noticed three very recent publications on the synthesis of ZnO nanocrystals using similar approaches: (a) Choi, S.-H.; Kim, E.-G.; Park, J.; An, K.; Lee, N.; Kim, S. C.; Hyeon, T. *J. Phys. Chem. B* **2005**, *109*, 14792−14794. (b) Andelman, T.; Gong, Y.; Polking, M.; Yin, M.; Kuskovsky, I.; Neumark, G.; O'Brien, S. *J. Phys. Chem. B* **2005**, *109*, 14314−14318. (c) Joo, J.; Kwon, S. G.; Yu, J. H.; Hyeon, T. *Adv. Mater.* **2005**, *17*, 1873−1877. Readers are encouraged to read these publications although this article does not solely concentrate on synthetic chemistry of ZnO nanocrystals.

Supporting Information Available: Additional figures and experimental details. This material is available free of charge via the Internet at http://pubs.acs.org.

JA053151G